Optical crosstalk in SPAD arrays for high-throughput single-molecule fluorescence spectroscopy

Antonino Ingargiola[a], Maya Segal[a], Angelo Gulinatti[b], Ivan Rech[b], Ivan Labanca[b], Piera Maccagnani[c], Massimo Ghioni[b], Shimon Weiss[a], Xavier Michalet[a]

[a]*Dep. of Chemistry and Biochemistry, University of California Los Angeles, USA*
[b]*Dip. di Elettronica, Informazione e Bioingegneria, Politecnico di Milano, Milan, Italy*
[c]*Istituto per la Microelettronica e Microsistemi, IMM-CNR, Bologna, Italy.*

Abstract

Single-molecule fluorescence spectroscopy (SMFS), based on the detection of individual molecules freely diffusing through the excitation spot of a confocal microscope, has allowed unprecedented insights into biological processes at the molecular level, but suffers from limited throughput. We have recently introduced a multispot version of SMFS, which allows achieving high-throughput SMFS by virtue of parallelization, and relies on custom silicon single-photon avalanche diode (SPAD) detector arrays [1]. Here, we examine the premise of this parallelization approach, which is that data acquired from different spots is uncorrelated. In particular, we measure the optical crosstalk characteristics of the two 48-SPAD arrays used in our recent SMFS studies, and demonstrate that it is negligible (crosstalk probability $\leq 1.1\ 10^{-3}$) and is undetectable in cross-correlation analysis of actual single-molecule fluorescence data.

Keywords: SPAD array, optical crosstalk, single-molecule, fluorescence, spectroscopy

1. Introduction

Single-molecule fluorescence spectroscopy includes several powerful techniques used to investigate fundamental physical, chemical and biological processes at the molecular level [2, 3, 4]. In its freely-diffusing molecule version, where molecules briefly transit (in a few ms) in and out of a confocal excitation spot, concentration needs to be kept low so that individual molecule "bursts" of photons can be identified. This results in long acquisition time (10 min to several hr) in order to accumulate sufficient statistics. To overcome this limitation, we use a multispot excitation/detection approach, and matching arrays of silicon single-photon avalanche diodes (SPAD) arrays [5, 6, 7, 1]. The number of photons in a burst is limited by the diffusion speed of typical biomolecules across the excitation volume, by the excitation power and by the photophysical properties (e.g. brightness) of the fluorophores used to label molecules of interest. Because of the low photon-count ($\sim$ 100) of typical bursts, SMFS requires SPADs with high photon-detection efficiency (PDE) in the visible range of the spectrum. For these reasons, our SPAD arrays are fabricated using a custom process, instead of the more common complementary metal-oxide semiconductor (CMOS) process [8, 9]. We recently demonstrated a SMFS system achieving close to 2-orders of magnitude throughput enhancement for single-molecule fluorescence resonant energy transfer (smFRET), using two excitation lasers and two 48-pixels SPAD arrays, to collect photons emitted by the "donor" and "acceptor" fluorophores attached to each molecule [1]. This approach can be used for real-time studies of kinetic processes and opens the way to applications of SMFS in medical diagnostics and drug discovery.

One of the assumptions of parallel data acquisition is that data acquired in each spot is uncorrelated (independent) from that acquired in others. In other words, each spot samples an independent volume of the solution of single molecules, and no molecules are observed in separate spots at different times. This assumption is verified in our experiments, where spots are separated by a few µm, which translates in negligible probability of observing a molecule in a nearby spot after it has been detected in an initial one. Note that molecules may get in and out of each individual spot a few times before wandering away, a recurrence phenomenon which can be used to study long term dynamics in single-molecules [10, 11].

A more subtle requirement for the independence of single-molecule measurements performed in nearby spots, is the absence of crosstalk. We can define crosstalk between two spots as the presence of a fraction of the signal of spot A in the signal measured in spot B. One source of crosstalk between spots is due to the collection of light emitted from spot A by SPAD B, supposed to detect signal only from B. This can be readily excluded for similar geometrical reasons as used above to exclude long term correlation between spots. A less obvious but well-known type of cause (see section 2) specific to SPAD arrays, is the occurrence of internal electronic or optical crosstalk between the pixel pairs. Electrical crosstalk is usually negligible in a well designed SPAD array. Crosstalk between spots, regardless of its origin, does show up in cross-correlation func-

Email addresses: `ingargiola.antonino@gmail.com` (Antonino Ingargiola), `michalet@chem.ucla.edu` (Xavier Michalet)

tions, and can potentially affect some single-molecule analysis.

In this paper, we describe an accurate method for optical crosstalk estimation (section 2) and use it to characterize the optical crosstalk in the two SPAD arrays used in our 48-spot SMFS setup [1] (section 3). We show that the low crosstalk of these devices has a negligible effect on single-molecule measurements.

Data and code availability. All raw data presented are freely available on Figshare (doi.org/10.6084/m9.figshare.5146096). Notebooks and code used for analysis and simulations are open source and available on GitHub github.com/tritemio/48-pixel-SPAD-crosstalk-analysis.

2. Optical crosstalk

Optical crosstalk between two SPADs within the same array can happen when an avalanche is triggered in one SPAD: hot carriers emit secondary photons [12, 13] which can propagate within the device structure, directly or after multiple reflections, and trigger an avalanche in another SPAD [14]. This secondary photons emission is proportional to the avalanche current [13] which typically lasts < 20 ns in SPADs using active quenching circuits [15]. Hence, when a crosstalk event occurs, the second SPAD is triggered with a delay < 20 ns. Optical crosstalk is a phenomenon present both in silicon (Si) custom [16], Si CMOS [17], III-V [18, 19] SPAD arrays and, particularly troublesome in Si photomultipliers (SiPM) [20, 21]. When the crosstalk probability is high (≥ 10%), cascades of multiple crosstalk events can be detected, although this is not usually an issue in Si SPAD arrays. In SiPM, where the signal from individual SPADs cannot be measured independently and the large crosstalk probability makes cascade effects non-negligible, optical crosstalk characterization is complex and requires sophisticated models [22, 21]. By contrast, in SPAD arrays, the crosstalk probability can be easily estimated by simple coincidence measurements as described next.

The crosstalk probability P_c can be estimated from the number of "coincidence events" , that is the number C of photons recorded within a given (short) time window Δt by two pixels A and B, over an acquisition duration T. Usually, crosstalk is estimated from dark counts acquisition, although, to reduce the acquisition time, SPADs can be also illuminated with a constant signal. The number of coincidences C can be measured with a dedicated asynchronous circuit [16, 17] or using the photon timestamps obtained with a simple counting board as used in single-molecule measurements. In this case, Δt needs to be chosen larger than the avalanche duration plus the time-stamp resolution (typically 10-20 ns).

The number of coincident events due to uncorrelated counts C_u can be computed from Poisson statistics, which we will assume to describe dark counts (similar expressions can be obtained for other statistics). Given two Poisson random variables $X_A \sim \text{Poi}\{\lambda_A \Delta t\}$ and $X_B \sim \text{Poi}\{\lambda_B \Delta t\}$ with mean event rate per unit time λ_A and λ_B, the probability of having at least one count in each variable during a time window Δt is:

$$P\{X_A \geq 1\}P\{X_B \geq 1\} = (1 - e^{\lambda_A \Delta t})(1 - e^{\lambda_B \Delta t}) \tag{1}$$

$$\approx \lambda_A \lambda_B (\Delta t)^2 \tag{2}$$

where the approximation holds when $\Delta t \ll \lambda^{-1}$. Hence, for two uncorrelated Poisson processes, the number of coincidences in Δt during a time T is:

$$C_u = P\{X_A \geq 1\}P\{X_B \geq 1\}\frac{T}{\Delta t} \tag{3}$$

The number of crosstalk events C_c can be computed as:

$$C_c = C - C_u \tag{4}$$

and the crosstalk probability as:

$$P_c = \frac{C_c}{N_A + N_B - C_c} \tag{5}$$

The standard deviation of the P_c estimator in eq. 5 can be computed from the standard deviation of C_c, which is a Poisson random variable as well (C_c counts are independent events):

$$\sigma_{P_c} = \frac{C_c^{1/2}}{N_A + N_B - C_c} \tag{6}$$

The rates λ_A, λ_B in eq. 1 can be estimated from dark counts measurements as:

$$\lambda_A = \frac{N_A - C_c}{T}\,, \qquad \lambda_B = \frac{N_B - C_c}{T} \tag{7}$$

where N_A and N_B are the total counts in SPAD A and B during duration T. Using eq. 7 in eq. 4 leads to an equation that can be solved for C_c, so that the probability of crosstalk and its standard deviation can be computed from eq. 5 and 6. The supporting notebook *Crosstalk Theory and Simulations* reports crosstalk simulations confirming that estimator in eq. 5 is unbiased.

3. Results and Discussion

We used eq. 1, 5, 6 and 7 with $\Delta t = 50$ ns to compute the crosstalk in the two 48-SPAD arrays used in ref. [1]. These arrays have a 12×4 geometry with 500 µm pitch and 50 µm diameter. In order to achieve accurate estimation, even for SPADs with very low dark count rates (DCR) (~50 cps, see ref. [1] for details), we acquired data for ~6 hours. Computational details can be found in the supporting notebook *Optical crosstalk estimation*.

Results in Fig. 1 show that the optical crosstalk probability P_c is $\sim 1.1\ 10^{-3}$ for nearest-neighbor SPADs, $\sim 1.5\ 10^{-4}$ for nearest-neighbor SPADs on a diagonal, and decreases by more than one order of magnitude down to negligible levels for SPADs farther apart. The crosstalk dependence with distance (Fig. 1, Panel A & D) indicates a much stronger absorption of secondary photons within the device compared to previous arrays [7, 14]. An R^{-2} dependence (black dashed curve) is indicated for comparison and corresponds to a simple isotropic

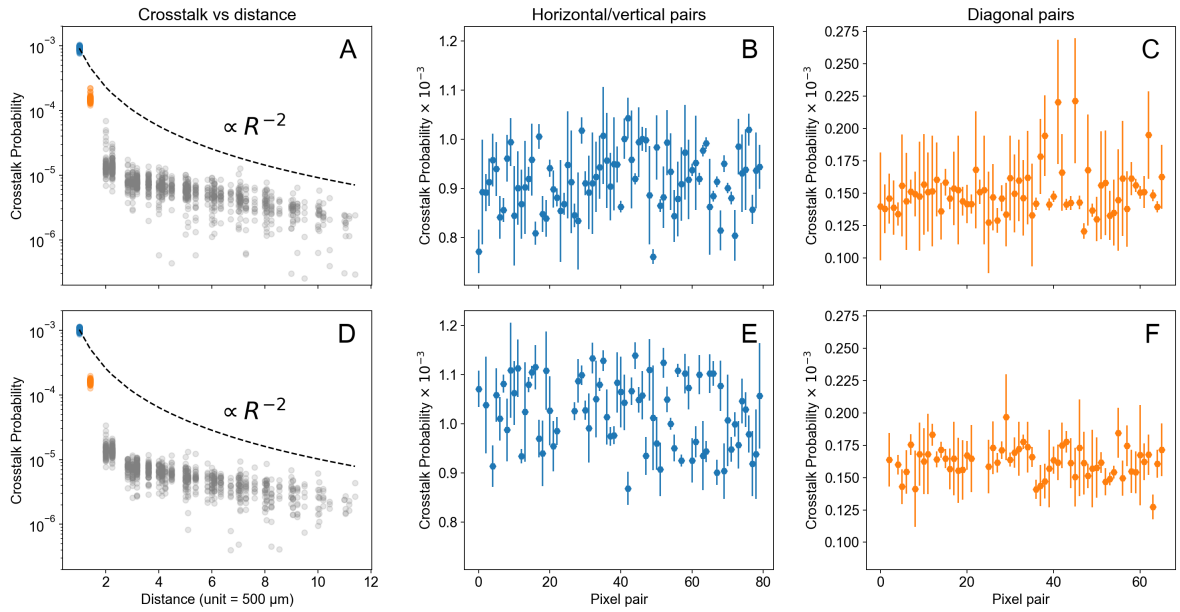

Figure 1: Optical crosstalk probability in the two 48-SPAD arrays used in our experiments. The two rows (A-C) and (D-F) present data from the "acceptor" and "donor" SPAD array respectively. Panels A,D show the crosstalk probability as a function of the distance between all pixel pairs. The black dashed line is a curve proportional to R^{-2} passing through the mean crosstalk of the nearest neighbor pairs (*blue dots*). The first two distances are color-coded and reported in detail in Panels B,E (nearest-neighbor pairs, 500 µm: *blue*) and Panel C,F (nearest diagonal neighbor pairs, $\sqrt{2}$ 500 µm: *orange*). Error bars in Panels B,C,E,F indicate the $\pm 3\sigma$ range, with σ computed according to eq. 6.

attenuation model, assuming direct propagation between pixels and no absorption. By contrast, crosstalk was observed to decrease slower than this simple R^{-2} model in a previous generation of SPAD arrays, an effect attributed to reflection of near infrared photons off the chip's bottom surface [14]. The stronger attenuation observed here has been obtained by fabricating the arrays on a silicon substrate with an especially high doping level ($> 2\ 10^{19}$ cm^{-3}). At these concentrations, free carriers absorption strongly reduces the propagation of near infrared photons through the substrate [23]. The good uniformity of crosstalk probability across both arrays also suggests that no edge effect is present in these devices, in contrast with the previous generation of devices [14]. Reflections off the chip edges, whose minimum distance from a SPAD is 450 µm, are made negligible by the strong reduction of the crosstalk with the distance.

These excellent crosstalk characteristics can be further observed in Fig. 2, which reports the auto-correlation and cross-correlation functions (ACF & CCF, eq. 8) of the donor intensity in 4 adjacent pixels during a typical smFRET measurement [1]. The curves have been computed with the open source Python package `pycorrelate`, using the algorithm from ref. [24]. See the supporting notebook *ACF and CCF* for details.

$$ACF(\tau) = \frac{\langle I(t+\tau)I(t)\rangle}{\langle I\rangle^2},\ CCF_{AB}(\tau) = \frac{\langle I_A(t+\tau)I_B(t)\rangle}{\langle I_A\rangle\langle I_B\rangle}. \quad (8)$$

Assuming an ideal Gaussian cylindrical profile for the excitation/detection probability, the ACF of a solution of freely diffusing molecules at equilibrium takes a simple form given by eq. 9 [25, 26].

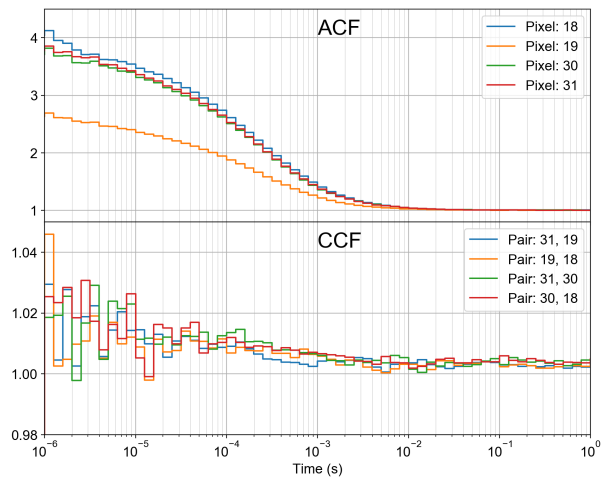

Figure 2: Normalized intensity auto- and cross-correlation functions for a group of 4 adjacent SPADs during a typical smFRET experiment.

$$ACF(\tau) = 1 + \frac{1}{N}(1 + SBR^{-1})^{-2}\left(1 + \frac{\tau}{\tau_D}\right)^{-1}. \quad (9)$$

In eq. 9, N is the average number of molecules present in the excitation/detection volume and SBR is signal-to-background ratio. This function exhibits a characteristic inflexion point around the diffusion time through the excitation/detection volume, τ_D, and ideally plateaus to a value $1/N$ at short time scale. In practice, additional contribution of the SPAD afterpulsing at short time scale (not shown) mask this asymptotic behavior [5].

In the absence of measurable molecular transport from one

spot to another, no correlation between the signals measured in the two different spots A and B is expected, and the CCF of the intensities recorded in the two spots, $CCF_{AB}(\tau)$ (eq. 8) should be equal to 1 (at least at time scales larger than ~ 1 µs). In the presence of crosstalk, an "echo" of the ACF of each spot is expected, whose amplitude is that of the ACF ($1/N$ in eq. 9) multiplied by the crosstalk probability, P_c. Fig. 2 is compatible with this prediction, the CCF amplitude (P_c/N) being smaller than the statistical noise level present in these (relatively) short measurements.

4. Conclusions

In this study, we have characterized the optical crosstalk of two large SPAD arrays used in single-molecule fluorescence experiments, and showed it to be extremely low. In particular, we have verified that it does not affect CCF analysis, a particularly useful property for high-throughput measurements in flow geometries. The ability to perform CCF analysis between distinct spots with negligible influence of crosstalk makes it practical to use these SPAD arrays for high-throughput SMFS measurements in flow geometries, where transport of molecules from one spot to another, and conformational change during that time, would result in non-trivial CCF signatures. Future work will take advantage of this possibility.

Acknowledgments: This work was funded by NIH Grant R01 GM095904. S. Weiss discloses intellectual property used in the research reported here. The work at UCLA was conducted in Dr. Weiss's Laboratory. M. Ghioni discloses equity in Micro Photon Devices S.r.l. (MPD). No resources or personnel from MPD were involved in this work. We are grateful to our colleagues at UCLA and Polimi for their contributions to this project over the years.

[1] Ingargiola, A., Segal, M., Gulinatti, A., Rech, I., Labanca, I., Maccagnani, P., et al. 48-spot single-molecule FRET setup with periodic acceptor excitation. bioRxiv 2017;:156182doi:10.1101/156182.

[2] Xie, X.S., Trautman, J.K.. Optical studies of single molecules at room temperature. Annu Rev Phys Chem 1998;49:441–480. doi:10.1146/annurev.physchem.49.1.441.

[3] Moerner, W.E., Orrit, M.. Illuminating Single Molecules in Condensed Matter. Science 1999;283(5408):1670–1676. doi:10.1126/science.283.5408.1670.

[4] Weiss, S.. Fluorescence spectroscopy of single biomolecules. Science (New York, NY) 1999;283(5408):1676–1683. doi:10.1126/science.283.5408.1676.

[5] Colyer, R.A., Scalia, G., Rech, I., Gulinatti, A., Ghioni, M., Cova, S., et al. High-throughput FCS using an LCOS spatial light modulator and an 8 × 1 SPAD array. Biomedical Optics Express 2010;1(5):1408–1431. doi:10.1364/BOE.1.001408.

[6] Ingargiola, A., Panzeri, F., Sarkosh, N., Gulinatti, A., Rech, I., Ghioni, M., et al. 8-spot smFRET analysis using two 8-pixel SPAD arrays. In: Proceedings of SPIE; vol. 8590. San Francisco, CA, USA; 2013, p. 85900E. doi:10.1117/12.2003704.

[7] Ingargiola, A., Lerner, E., Chung, S., Panzeri, F., Gulinatti, A., Rech, I., et al. Multispot single-molecule FRET: High-throughput analysis of freely diffusing molecules. PLOS ONE 2017;12(4):e0175766. doi:10.1371/journal.pone.0175766.

[8] Michalet, X., Ingargiola, A., Colyer, R.A., Scalia, G., Weiss, S., Maccagnani, P., et al. Silicon Photon-Counting Avalanche Diodes for Single-Molecule Fluorescence Spectroscopy. IEEE Journal of Selected Topics in Quantum Electronics 2014;20(6):1–20. doi:10.1109/JSTQE.2014.2341568.

[9] Bruschini, C., Homulle, H., Charbon, E.. Ten years of biophotonics single-photon SPAD imager applications: Retrospective and outlook. vol. 10069. International Society for Optics and Photonics; 2017, p. 100691S. doi:10.1117/12.2256247.

[10] Hoffmann, A., Nettels, D., Clark, J., Borgia, A., Radford, S.E., Clarke, J., et al. Quantifying heterogeneity and conformational dynamics from single molecule FRET of diffusing molecules: Recurrence analysis of single particles (RASP). Physical Chemistry Chemical Physics 2011;13(5):1857–71. doi:10.1039/c0cp01911a.

[11] Pirchi, M., Tsukanov, R., Khamis, R., Tomov, T.E., Berger, Y., Khara, D.C., et al. Photon-by-Photon Hidden Markov Model Analysis for Microsecond Single-Molecule FRET Kinetics. J Phys Chem B 2016;120(51):13065–13075. doi:10.1021/acs.jpcb.6b10726.

[12] Bude, J., Sano, N., Yoshii, A.. Hot-carrier luminescence in Si. Phys Rev B 1992;45(11):5848–5856. doi:10.1103/PhysRevB.45.5848.

[13] Lacaita, A.L., Zappa, F., Bigliardi, S., Manfredi, M.. On the bremsstrahlung origin of hot-carrier-induced photons in silicon devices. IEEE Transactions on Electron Devices 1993;40(3):577–582. doi:10.1109/16.199363.

[14] Rech, I., Ingargiola, A., Spinelli, R., Labanca, I., Marangoni, S., Ghioni, M., et al. Optical crosstalk in single photon avalanche diode arrays: A new complete model. Opt Express, OE 2008;16(12):8381–8394. doi:10.1364/OE.16.008381.

[15] Gallivanoni, A., Rech, I., Ghioni, M.. Progress in Quenching Circuits for Single Photon Avalanche Diodes. IEEE Transactions on Nuclear Science 2010;57(6):3815–3826. doi:10.1109/TNS.2010.2074213.

[16] Restelli, A., Rech, I., Maccagnani, P., Ghioni, M., Cova, S.. Monolithic silicon matrix detector with 50 µm photon counting pixels. Journal of Modern Optics 2007;54(2-3):213–223. doi:10.1080/09500340600790121.

[17] Ficorella, A., Pancheri, L., Betta, G.F.D., Brogi, P., Collazuol, G., Marrocchesi, P.S., et al. Crosstalk mapping in CMOS SPAD arrays. In: 2016 46th European Solid-State Device Research Conference (ESSDERC). 2016, p. 101–104. doi:10.1109/ESSDERC.2016.7599598.

[18] Calandri, N., Sanzaro, M., Motta, L., Savoia, C., Tosi, A.. Optical Crosstalk in InGaAs/InP SPAD Array: Analysis and Reduction With FIB-Etched Trenches. IEEE Photonics Technology Letters 2016;28(16):1767–1770. doi:10.1109/LPT.2016.2570278.

[19] Piccione, B., Jiang, X., Itzler, M.A.. Spatial modeling of optical crosstalk in InGaAsP Geiger-mode APD focal plane arrays. Opt Express, OE 2016;24(10):10635–10648. doi:10.1364/OE.24.010635.

[20] Buzhan, P., Dolgoshein, B., Ilyin, A., Kaplin, V., Klemin, S., Mirzoyan, R., et al. The cross-talk problem in SiPMs and their use as light sensors for imaging atmospheric Cherenkov telescopes. Nuclear Instruments and Methods in Physics Research Section A: Accelerators, Spectrometers, Detectors and Associated Equipment 2009;610(1):131–134. doi:10.1016/j.nima.2009.05.150.

[21] Seifert, S., van Dam, H.T., Vinke, R., Dendooven, P., Lohner, H., Beekman, F.J., et al. A Comprehensive Model to Predict the Timing Resolution of SiPM-Based Scintillation Detectors: Theory and Experimental Validation. IEEE Transactions on Nuclear Science 2012;59(1):190–204. doi:10.1109/TNS.2011.2179314.

[22] Gallego, L., Rosado, J., Blanco, F., Arqueros, F.. Modeling crosstalk in silicon photomultipliers. J Inst 2013;8(05):P05010. doi:10.1088/1748-0221/8/05/P05010.

[23] Spitzer, W., Fan, H.Y.. Infrared Absorption in n-Type Silicon. Phys Rev 1957;108(2):268–271. doi:10.1103/PhysRev.108.268.

[24] Laurence, T.A., Fore, S., Huser, T.. Fast, flexible algorithm for calculating photon correlations. Opt Lett, OL 2006;31(6):829–831. doi:10.1364/OL.31.000829.

[25] Krichevsky, O., Bonnet, G.. Fluorescence correlation spectroscopy: The technique and its applications. Rep Prog Phys 2002;65(2):251. doi:10.1088/0034-4885/65/2/203.

[26] Michalet, X., Colyer, R.A., Scalia, G., Ingargiola, A., Lin, R., Millaud, J.E., et al. Development of new photon-counting detectors for single-molecule fluorescence microscopy. Philosophical Transactions of the Royal Society B: Biological Sciences 2012;368(1611):1–22. doi:10.1098/rstb.2012.0035.